A phase 3 non-inferiority study of 5-FU/l-leucovorin/irinotecan (FOLFIRI) versus irinotecan/S-1 (IRIS) as second-line chemotherapy for metastatic colorectal cancer: updated results of the FIRIS study. J Cancer Res Clin Oncol.2015;141: 153-160

4) Hirano G, Makiyama A,Makiyama C,Esaki T,Oda H,Uchino K,Komoda M,Tanaka R,Matsushita Y,Mitsugi K,Shibata Y,Kumagai H, Arita S,Ariyama H,Kusaba H,Akashi K, Baba E. Reduced Dose of Salvage-line Regorafenib Monotherapy for Metastatic Colorectal Cancer in Japan. Anticancer Research. 2015;35: 371-377

2. 学会発表

1) Hironaka S,Shimada Y,Sugimoto N,Komatsu Y,Nishina T,Yamaguchi K,Segawa Y,Omuro Y,Tamura T,Doi T,Yukisawa S,Yasui H,Nagashima F,Gotoh M,Esaki T,Emig M,Chandrawansa K,Muro K,Wilke H,Ohtsu A. RAINBOW:A global,phase Ⅲ,randomized,double-blind study of ramucirumab(RAM)plus paclitaxel(PTX)versus placebo(PL)plus PTX in the treatment of metastatic gastroesophageal junction and gastric adenocarcinoma(mGC)following disease progression on first-line platinum -and fluoropyrimidine-containing combination therapy-Efficacy analysis in Japanese and Western patients. 2014 Annual Meeting of the American Society of Clinical Oncology. Chicago. 140530-0603

2) Yamaguchi K,Hironaka S,Sugimoto N,Moriwaki T,Komatsu Y,Nishina T,Tsuji A,Nakajima T,Gotoh M,Machida N,Fuse N,Esaki T,Emi Y,Takinishi Y,Matsumoto S,Boku N,Baba H,Hyodo I. Randomized phase Ⅱ study of S-1 plus oral leucovorin(SL)versus SL plus Oxaliplatin(SOL)versus S-1 plus cisplatin(SP)in patients with advanced gastric cancer(AGC):updated overall survival data. 2014 Europian society for medical oncology. Madrid. 140926-140930

H. 知的財産権の出願・登録状況 (予定を含む)

1. 特許取得

なし

2. 実用新案登録

なし

3. その他

なし

厚生労働科学研究費補助金
がん対策推進総合研究事業（革新的がん医療実用化研究事業）
腹腔内転移癌を対象としたＨＢ-ＥＧＦを分子標的とするがん治療薬ＢＫ-ＵＭの第２相試験
分担研究報告書

初回化学療法不応の腹膜播種を有する進行・再発胃癌を対象とした，HB-EGF特異的抑制剤BK-UMとパクリタキセル少量分割併用療法の第I/II相臨床試験

研究分担者　辻　晃仁　神戸市立医療センター中央市民病院　腫瘍内科部長

研究要旨：BK-UMとパクリタキセル少量分割療法を被験治療とした，単アーム多施設共同非盲検試験とし，プロトコル治療の有効性がヒストリカルデータ（JCOG0407試験治療のパクリタキセル単独治療群）より優れている可能性を検証する。

A．研究目的

BK-UM とパクリタキセル少量分割療法を被験治療とした，単アーム多施設共同非盲検試験デザインとし，プロトコル治療の有効性がヒストリカルデータ（JCOG0407 試験治療のパクリタキセル単独治療群）より優れている可能性を検証する。

B．研究方法

治験デザイン：第 I/II 相試験。本治験は，BK-UM とパクリタキセル少量分割投与をプロトコル治療とする，多施設共同非盲検デザインとする。

対象：初回化学療法としてフッ化ピリミジン系抗癌剤を投与されたにもかかわらず，腹腔内に播種・転移を示した進行・再発胃癌患者を対象とする。

目標症例数：最大 42 例（第 I 相部 3 例～12 例，第 II 相部の推奨用量投与患者は，30 例とする。）

適格基準：以下の条件を全て満たす場合のみ，本治験の組み入れ対象とする。

(1) 組織学的に胃原発の腺癌（組織型分類の一般型のいずれか）であることが確認されている患者
(2) 切除不能胃癌または再発胃癌である患者
(3) 腹膜転移を有する患者（腹膜以外の他臓器への転移の有無及び測定可能病変の有無は問わない。）
(4) ECOG Performance Status (PS) が 0，1，2 の患者
(5) 次の①，②のいずれか一方に該当する患者（①と②両方に該当する場合は不適格とする。）
　① 4 週間以上継続されたフッ化ピリミジン系抗癌剤を含む術後補助化学療法が，投与中もしくは最終抗癌剤投与日から 24 週以内に臨床的に増悪と判断されて中止された（術前化学療法から継続して施行されている症例を含む）
　② 術後補助化学療法ではない，4 週間以上継続されたフッ化ピリミジン系抗癌剤を含む初回化学療法が，投与中もしくは最終抗癌剤投与日から 4 週間以内に臨床的に増悪と判断されて中止※注 2 された
(6) 腹腔内投与を行うため，腹腔内へのポートの留置可能な患者
(7) 十分な主要臓器能を保持している患者（検査値は登録前 14 日以内の値とする）
　① 白血球数　3,000/mm3 以上　かつ 12,000/ mm3 以下
　② 血小板数　100,000/mm3 以上
　③ ヘモグロビン　8.0g/dL 以上
　④ AST　100U/L（IU/l）以下
　⑤ ALT　100U/L（IU/l）以下
　⑥ 血清総ビリルビン　1.5mg/dL 以下
　⑦ 血清クレアチニン　1.5mg/dL 以下
　⑧ CRP　10mg/dL 以下
　⑨ 心機能障害：治療を要する心疾患のない患者
　⑩ 神経障害：Grade 3 以上の神経障害を認めない患者
(8) 同意取得時，年齢 20 歳以上 75 歳以下の患者
(9) 胃癌以外の悪性腫瘍に対する抗癌剤による化学療法，または胃癌を含む悪性腫瘍に対する放射線療法の既往がない患者
(10) 本治験への参加につき，本人から自由意思

による文書同意が得られた患者

治験参加施設
九州大学病院　消化管外科（2）
福岡大学病院　腫瘍・血液・感染症内科
済生会福岡総合病院　外科
九州医療センター　がん臨床研究部
九州がんセンター　消化管・腫瘍内科
神戸市立医療センター　腫瘍内科
愛知県がんセンター中央病院　薬物療法部
東京大学医科学研究所附属病院　外科

（倫理面への配慮）
治験責任医師及び治験に係わるすべての関係者は，ヘルシンキ宣言に基づく倫理的原則，薬事法，GCP 及び関連する通知，並びに本治験実施計画書に従って治験を実施する。

C．研究結果
現在、プロトコールが完成し、3 月 20 日に九州医療センターでの治験倫理審査委員会の承認後、治験届けを提出した。

D．考察
本邦における癌による死亡の原因として，胃癌は肺癌に次ぐ第 2 位となっている。胃癌の罹患率は過去と比べると減少しているものの，胃癌の発生率は依然として高く，胃癌罹患者数は年間約 10 万人，死亡者数は約 5 万人である。
現在，切除不能あるいは再発胃癌には初回治療としてフッ化ピリミジン系抗癌剤を含む化学療法が標準治療として行われている。日本人を対象として行われた SPIRITS 試験では現在の標準治療が S-1 及びシスプラチンの併用療法であることが決定づけられたが，その効果は十分とは言えず，S-1 及びシスプラチン併用患者の生存期間中央値 13 ヵ月，無増悪生存期間は 6.0 ヶ月，1 年生存率は 54.1％である。海外で行われた FLAGS 試験によると，S-1 及びシスプラチン併用患者の生存期間中央値は 8.6 ヵ月，無増悪生存期間 4.8 ヶ月，1 年生存率は 40％以下であった。
一方，胃癌の転移，再発形式には播種性，リンパ行性，血行性と大きく 3 つの経路が知られている。この中でも最も頻度が高く，予後を左右する転移・再発形式が腹膜播種である。腹膜播種は，癌細胞が胃壁の外へ浸潤し，腹膜に多数拡散するように転移した状態である。腹膜播種は，腹水貯留，消化管閉塞などをきたすため，患者の QOL（生活の質）を著しく低下させるとともに，予後を悪化させる重要な因子となる。しかしながら腹膜播種のみを対象とした治療法の開発は最近まで行われておらず，これまでの胃癌に対する臨床試験の多くは，高度の腹膜播種症例を対象としていない。JCOG0106 試験は画像上の腹膜播種がある症例に対して 5-FU の持続静注療法と 5-FU/Methotrexate 療法を比較した唯一の PhaseIII 試験であるが，経口摂取可能例の 1 年生存率は，30.1%から 33.3%と極めて低い。このように明らかな腹膜播種を呈する症例の予後は極めて悪いことが予想されている。現在腹膜播種症例を対象とした 2 つの PhaseIII 試験が行われており、Phoenix-GC 試験は腹膜播種初回治療例を対象として現在の標準治療である S-1/CDDP 併用療法と S-1/パクリタキセル静注および腹腔内併用療法を比較しており，既に登録が終了している。また，さらに予後の悪い高度の腹膜播種の初回治療例を対象として，5-FU/l-LV 療法 vs。 FLTAX（5-FU/l-LV+PTX）療法のランダム化第 II/III 相比較試験が JCOG1108 試験として行われている。本試験ではこれまでほとんど行われていない初回治療を行った後の腹膜播種症例を対象とした試験を計画した。

E．結論
前臨床試験が終了とほぼ同時進行で臨床治験開始の準備を行い、神戸市立医療センター中央市民病院では 3 月 IRB 審査施行。治験が開始できる状況となった。

F．健康危険情報
特記事項なし。

G．研究発表
1．論文発表

1） Hironaga Satake, Akihito Tsuji, Takeshi Kotake, Mikio Fujita　Feasibility of Outpatient Chemotherapy with S-1 and Cisplatin for Gastric Cancer Journal of Cancer Therapy, 2014, 5, 759-765
2） Daisuke Takahari, Narikazu Boku, Junki Mizusawa, Atsuo Takashima, YasuhideYamada, Takayuki Yoshino, Kentaro Yamazaki, Wasaburo Koizumi, Kazutoshi Fukase, Kensei Yamaguchi, Masahiro Goto, Tomohiro Nishina, Takao Tamura,Akihito Tsuji and Atsushi Ohtsu Determination of Prognostic Factors in Japanese Patients With AdvancedGastric Cancer Using the Data From a Randomized Controlled Trial, JapanClinical Oncology Group 9912 The Oncologist published online March 25, 2014

2．学会発表

1） Toshikazu Moriwaki, Shuichi Hironaka, Naotoshi Sugimoto, Kensei Yamaguchi, Yoshito Komatsu, Tomohiro Nishina, Akihito Tsuji, Narikazu Boku, Hideo Baba, Ichinosuke Hyodo.Randomized phase II study of S-1+leucovorin (SL) vs. SL+oxaliplatin (SOL) vs. S-1+cisplatin for advanced gastric cancer20140718 福岡市　第 12 回日本臨床腫瘍学会学術集会

H. 知的財産権の出願・登録状況 (予定を含む)

1. 特許取得

なし

2. 実用新案登録

なし

3. その他

なし

Ⅲ.　研究成果の刊行に関する一覧表

研究成果の刊行に関する一覧表

雑 誌

発表者氏名	論文タイトル名	発表誌名	巻号	ページ	出版年
Suzuki K, Mizushima H, Abe H, Iwamoto R, Nakamura H, Mekada E.	Identification of diphtheria toxin R domain mutants with enhanced inhibitory activity against HB-EGF	J Biochem.		In press	2014
Nam SO, Yotsumoto F, Miyata K, Suzaki Y, Yagi H, Odawara T, Manabe S, Ishikawa T, Kuroki M, Mekada E, Miyamoto S.	Pre-clinical study of BK-UM, a novel inhibitor of HB-EGF, for ovarian cancer therapy	Anticancer Res.	34(8)	4615-4620	2014
Okamoto A, Asai T, Kato H, Ando H, Minamino T, Mekada E, Oku N.	Antibody-modified lipid nanoparticles for selective delivery of siRNA to tumors expressing membrane-anchored form of HB-EGF	Biochem Biophys Res Commun.	449(4)	460-465	2014
Ando K, Oki E, Zhao Y, Ikawa-Yoshida A, Kitao H, Saeki H, Kimura Y, Ida S, Morita M, Kusumoto T, Maehara Y	Mortalin is a prognostic factor of gastric cancer with normal p53 function	Gastric Cancer	17	255-262	2014
Honma K, Nakanishi R, Nakanoko T, Ando K, Saeki H, Oki E, Iimori M, Kitao H, Kakeji Y, Maehara Y	Contribution of Aurora-A and -B expression to DNA aneuploidy in gastric cancers	Surg Today	44	454-461	2014
Baba Y, Watanabe M, Murata A, Shigaki H, Miyake K, Ishimoto T, Iwatsuki M, Iwagami S, Yoshida N, Oki E, Sakamaki K, Nakao M, Baba H.	LINE-1 hypomethylation, DNA copy number alterations, and CDK6 amplification in esophageal squamous cell carcinoma	Clin Cancer Res	20	1114-1124	2014
Kimura Y, Oki E, Yoshida A, Aishima S, Zaitsu Y, Ohtsu H, Ando K, Ida S, Saeki H, Morita M, Kusumoto T, Oda Y, Maehara Y.	Significance of accurate human epidermal growth factor receptor-2 (HER2) evaluation as a new biomarker in gastric cancer	Anticancer Res	33	4207-4212	2014
Oki E, Emi Y, Kusumoto T, Sakaguchi Y, Yamamoto M, Sadanaga N, Shimokawa M, Yamanaka T, Saeki H, Morita M, Takahashi I, Hirabayashi N, Sakai K, Orita H, Aishima S, Kakeji Y, Yamaguchi K, Yoshida K, Baba H, Maehara Y.	Phase II study of docetaxel and S-1 (DS) as neoadjuvant chemotherapy for clinical stage III resectable gastric cancer	Ann Surg Oncol	21	2340-2346	2014
Zaitsu Y, Oki E, Ando K, Ida S, Kimura Y, Saeki H, Morita M, Hirahashi M, Oda Y, Maehara Y.	Loss of Heterozygosity of PTEN (Encoding Phosphate and Tensin Homolog) Associated with Elevated HER2 Expression Is an Adverse Prognostic Indicator in Gastric Cancer	Oncology	88	189-194	2015
Masuda T, Nakashima Y, Ando K, Yoshinaga K, Saeki H, Oki E, Morita M, Oda Y, Maehara Y.	Nuclear expression of chemokine receptor CXCR4 indicates poorer prognosis in gastric cancer	Anticancer Res	34	6397-6403	2014

Ando K, Oki E, Saeki H, Yan Z, Tsuda Y, Hidaka G, Kasagi Y, Otsu H, Kawano H, Kitao H, Morita M, Maehara Y.	Discrimination of p53 immunohistochemistry-positive tumors by its staining pattern in gastric cancer	Cancer Med	4(1)	75-83	2015
Miyata K, Yotsumoto F, Nam SO, Odawara T, Manabe S, Ishikawa T, Itamochi H, Kigawa J, Takada S, Asahara H, Kuroki M, Miyamoto S.	Contribution of transcription factor, SP1, to the promotion of HB-EGF expression in defense mechanism against the treatment of irinotecan in ovarian clear cell carcinoma	Cancer Medicine	3	1159-1169	2014
Sasaki T, Kuniyasu H, Luo Y, Kitayoshi M, Tanabe E, Kato D, Shinya S, Fujii K, Ohmori H, Yamashita Y.	AKT Activation and Telomerase Reverse Transcriptase Expression are Concurrently Associated with Prognosis of Gastric Cancer	Pathobiology	81	36-41	2014
Shibata R, Nimura S, Hashimoto T, Miyake T, Takeno S, Hoshino S, Nabeshima K, Yamashita Y.	Expression of human epidermal growth factor receptor 2 in primary and paired parenchymal recurrent and/or metastatic sites of gastric cancer	Molecular and Clinical Oncology	2	751-755	2014
Takeno S, Hashimoto T, Maki K, Shibata R, Shiwaku H, Yamana I, Yamashita R, Yamashita Y.	Gastric cancer arising from the remnant stomach after distal gastrectomy: A review	World J Gastroenterology	20(38)	13734-40	2014
Yasui H, Tsurita G, Imai K.	DNA synthesis inhibitors for the treatment of gastrointestinal cancer	Expert Opin. Pharmacother	15(16)	2361-72	2014
Shigematsu A, Kobayashi N, Yasui H, Shindo M, Kakinoki Y, Koda K, Iyama S, Kuroda H, Tsutsumi Y, Imamura M, Teshima T.	High level of serum soluble interleukin-2 receptor at transplantation predicts poor outcome of allogeneic stem cell transplantation for adult T cell leukemia	Biol Blood Marrow Transplant	20(6)	801-5	2014
Takeuchi M, Sato Y, Yasui H, Ozawa H, Ohno K, Takata K, Iwaki N, Orita Y, Asano N, Nakamura S, Swerdlow SH, Yoshino T.	Epstein-Barr virus-infected cells in IgG4-related lymphadenopathy with comparison with extranodal IgG4-related disease	Am J Surg Pathol.	38(7)	946-55	2014
Imai K, Emi Y, Iyama K, Beppu T, Ogata Y, Kakeji Y, Samura H, Oki E, Akagi Y, Maehara Y, Baba H.	Splenic volume may be a useful indicator of the protective effect of bevacizumab against oxaliplatin-induced hepatic sinusoidal obstruction syndrome	Eur J Surg Oncology	40	559-566	2014
Beppu T, Emi Y, Tokunaga S, Oki E, Shirabe K, Ueno S, Kuramoto M, Kabashima A, Takahashi I, Samura H, Eguchi S, Akagi Y, Natsugoe S, Ogata Y, Kakeji Y, Baba H, Maehara Y; Kyushu Study group of Clinical Cancer (KSCC).	Liver resectability of advanced liver-limited colorectal liver metastases following mFOLFOX6 with bevacizumab (KSCC0802 Study)	Anticancer Res.	34(11)	6655-62	2014
Kang YK, Muro K, Ryu MH, Yasui H, Nishina T, Ryoo BY, Kamiya Y, Akinaga S, Boku N.	A phase II trial of a selective c-Met inhibitor tivantinib(ARQ 197) monotherapy as a second- or third-line therapy in the patients with metastatic gastric cancer	Invest New Drugs	32(2)	355-61	2014

Boku N, Muro K, Machida N, Hashigaki S, Kimura N, Suzuki M, Lechuga M, Miyata Y.	Phase I study of sunitinib plus S-1 and cisplatin in Japanese patients with advanced or metastatic gastric cancer	Invest New Drugs	32(2)	261-70	2014
Shitara K, Matsuo K, Muro K, Doi T, Ohtsu A.	Correlation between overall survival and other endpoints in clinical trials ofsecond-line chemotherapy for patients with advanced gastric cancer	Gastric Cancer	17(2)	362-70	2014
Kodera Y, Fujitani K,Fukushima N, Ito S, Muro K, Ohashi N, Yoshikawa T, Kobayashi D, Tanaka C, Fujiwara M.	Surgical resection of hepatic metastasis from gastric cancer:a review and new recommendation in the Japanese gastric cancer treatment guidelines	Gastric Cancer	17(2)	206-12	2014
Sasaki Y, Nishina T, Yasui H, Goto M, Muro K, Tsuji A, Koizumi W, Toh Y, Hara T, Miyata Y.	Phase II trial of nanoparticle albumin-bound paclitaxel as second-line chemotherapy for unresectable or recurrent gastric cancer	Cancer Sci	105(7)	812-7	2014
Kadowaki S, Komori A, Narita Y, Nitta S, Yamaguchi K, Kondo C, Taniguchi H, Takahari D, Ura T, Ando M, Muro K.	Long-term outcomes and prognostic factors of patients with advanced gastric cancer treated with S-1 plus cisplatin combination chemotherapy as a first-line treatment	Int J Clin Oncol	19(4)	656-61	2014
Wilke H, Muro K, Van Cutsem E, Oh SC, Bodoky G, Shimada Y, Hironaka S, Sugimoto N, Lipatov O, Kim TY, Cunningham D, Rougier P, Komatsu Y, Ajani J, Emig M, Carlesi R, Ferry D, Chandrawansa K, Schwartz JD, Ohtsu A; RAINBOW Study Group	Ramucirumab plus paclitaxel versus placebo plus paclitaxel in patients with previously treated advanced gastric or gastro-oesophageal junction adenocarcinoma (RAINBOW): a double-blind, randomised phase 3 trial	Lancet Oncol	15(11)	1224-35	2014
Ando K, Oki E, Ikeda T, Saeki H, Ida S, Kimura Y, Soejima Y, Morita M, Shirabe K, Kusumoto T, Maehara Y.	Simultaneous resection of colorectal cancer and liver metastases in the right lobe using pure laparoscopic surgery	Surg Today	44(8)	1588-92	2014
Taketani K, Tokunaga E, Yamashita N, Tanaka K, Akiyoshi S, Okada S, Ando K, Kimura Y, Saeki H, Oki E, Morita M, Kusumoto T, Maehara Y.	The early discontinuation of adjuvant hormone therapy is associated with a poor prognosis in Japanese breast cancer patients	Surg Today	44(10)	1841-6	2014
Morita M, Otsu H, Kawano H, Kasagi Y, Kimura Y, Saeki H, Ando K, Ida S, Oki E, Tokunaga E, Ikeda T, Kusumoto T, Maehara Y.	Gender differences in prognosis after esophagectomy for esophageal cancer	Surg Today	44(3)	505-12	2014
Ida S, Oki E, Ando K, Kimura Y, Yamashita Y, Saeki H, Ikegami T, Yoshizumi T, Watanabe M, Morita M, Shirabe K, Kusumoto T, Ikeda T, Baba H, Maehara Y.	Pure laparoscopic right-sided hepatectomy in the semi-prone position for synchronous colorectal cancer with liver metastases	Asian J Endosc Surg	7(2)	133-7	2014

Ida S, Morita M, Hiyoshi Y, Ikeda K, Ando K, Kimura Y, Saeki H, Oki E, Kusumoto T, Yoshida S, Nakashima T, Watanabe M, Baba H, Maehara Y.	Surgical resection of hypopharynx and cervical esophageal cancer with a history of esophagectomy for thoracic esophageal cancer	Ann Surg Oncol	21(4)	1175-81	2014
Isobe T, Uchino K, Makiyama C, AriyamaH, Arita S, Tamura S, Komoda M, Kusaba H, Shirakawa T, Esaki T, Mitsugi K, Takaishi S, Akashi K, Baba E.	Analysis of adverse events of bevacizumab-containing systemic chemotherapy for metastatic colorectal cancer inJapan	Anticancer Research	34(4)	2035-2040	2014
Yasui H, Muro K, Shimada Y, Tsuji A, Sameshima S, Baba H, Satoh T, Denda T, Ina K, Nishina T, Yamaguchi K, Esaki T, Tokunaga S, Kuwano H, Boku N, Komatsu Y, Watanabe M, Hyodo I, Morita S, Sugihara K.	A phase 3 non-inferiority study of 5-FU/l-leucovorin/irinotecan (FOLFIRI) versus irinotecan/S-1 (IRIS) as second-line chemotherapy for metastatic colorectal cancer: updated results of the FIRIS study	J Cancer Res Clin Oncol	141	153-160	2015
HiranoG,MakiyamaA,Makiyama C,EsakiT,OdaH,UchinoK, Komoda M,Tanaka R,Matsushita Y,Mitsugi K,Shibata Y,Kumagai H, Arita S,Ariyama H,Kusaba H,Akashi K, Baba E.	Reduced Dose of Salvage-line Regorafenib Monotherapy for Metastatic Colorectal Cancer in Japan	Anticancer Research	35	371-377	2015
Hironaga Satake, Akihito Tsuji, Takeshi Kotake, Mikio Fujita.	Feasibility of Outpatient Chemotherapy with S-1 and Cisplatin for Gastric Cancer	Journal of Cancer Therapy	5	759-765	2014

Ⅳ.　研究成果の別刷

J. Biochem. 2014;1–13 doi:10.1093/jb/mvu079 Journal of Biochemistry Advance Access published December 20, 2014 THE JOURNAL OF BIOCHEMISTRY

Identification of diphtheria toxin R domain mutants with enhanced inhibitory activity against HB-EGF

Received September 29, 2014; accepted October 21, 2014; published online November 27, 2014

Keisuke Suzuki[1], Hiroto Mizushima[1], Hiroyuki Abe[2], Ryo Iwamoto[1], Haruki Nakamura[3] and Eisuke Mekada[1,*]

[1]Department of Cell Biology and [2]Department of Molecular Bacteriology, Research Institute for Microbial Diseases, Osaka University, 3-1 Yamadaoka, Suita, Osaka 565-0871, Japan; and [3]Institute for Protein Research, Osaka University, 3-2 Yamadaoka, Suita, Osaka 565-0871, Japan

*Eisuke Mekada, Department of Cell Biology, Research Institute for Microbial Diseases, Osaka University, 3-1 Yamadaoka, Suita, Osaka 565-0871, Japan. Tel: +81-6-6879-8286, Fax: +81-6-6879-8289, email: emekada@biken.osaka-u.ac.jp

Heparin-binding epidermal growth factor-like growth factor (HB-EGF), a ligand of EGF receptor, is involved in the growth and malignant progression of cancers. Cross-reacting material 197, CRM197, a non-toxic mutant of diphtheria toxin (DT), specifically binds to the EGF-like domain of HB-EGF and inhibits its mitogenic activity, thus CRM197 is currently under evaluation in clinical trials for cancer therapy. To develop more potent DT mutants than CRM197, we screened various mutant proteins of R domain of DT, the binding site for HB-EGF. A variety of R-domain mutant proteins fused with maltose-binding protein were produced and their inhibitory activity was evaluated *in vitro*. We found four R domain mutants that showed much higher inhibitory activity against HB-EGF than wild-type (WT) R domain. These R domain mutants suppressed HB-EGF-dependent cell proliferation more effectively than WT R domain. Surface plasmon resonance revealed their higher affinity to HB-EGF than WT R domain. CRM197(R460H) carrying the newly identified mutation showed increased cell proliferation inhibitory activity and affinity to HB-EGF. These results suggest that CRM197(R460H) or other recombinant proteins carrying newly identified mutation(s) in the R domain are potential therapeutics targeting HB-EGF.

Keywords: cancer/CRM197/diphtheria toxin/EGF receptor/HB-EGF.

Abbreviations: BHI, brain heart infusion; BRL, Buffalo rat liver; CM, conditioned medium; CRM197, cross-reacting material 197; 3D, three dimensional; DT, diphtheria toxin; DLT, diphtheria-like toxin; FBS, foetal bovine serum; GST, glutathione-S-transferase; HB-EGF, heparin-binding epidermal growth factor-like growth factor; HEPES, 4-(2-Hydroxyethyl)-1-piperazineethane-sulfonic acid; IPTG, isopropyl β-D-1-thiogalactopyranoside; MBP, maltose-binding protein; PMSF, phenylmethylsulfonyl fluoride; PCR, polymerase chain reaction; sHB-EGF, soluble HB-EGF; siRNA, short interfering RNA; TGF-α, transforming growth factor-α; TRX, thioredoxin; WT, wild-type.

The epidermal growth factor (EGF) family, which includes EGF, transforming growth factor-α (TGF-α), heparin-binding EGF-like growth factor (HB-EGF), amphiregulin, epiregulin, β-cellulin, epigen and neuregulin1-4, activates ErbB family receptors. Members of this family are synthesized as membrane-anchored precursor proteins (*1*). These precursor proteins are cleaved by ADAM family metalloproteases such as ADAM9, ADAM10, ADAM12 and ADAM17 by a mechanism called ectodomain shedding to release soluble ligands that activate receptors in a paracrine fashion (*2*, *3*).

HB-EGF was identified as a ligand for EGF receptor (EGFR/ErbB1) with heparin-binding properties (*4*, *5*). ProHB-EGF is cleaved within the juxtamembrane domain on the cell surface, resulting in the shedding of soluble HB-EGF (sHB-EGF). HB-EGF also binds and activates ErbB4 (*6*). sHB-EGF is a potent mitogen and chemoattractant for a number of cell types including vascular smooth muscle cells, fibroblasts and keratinocytes (*7*) and a recent study indicated that the proliferation-promoting activity of HB-EGF is especially evident in culture systems in which cell-matrix adhesion is reduced (*8*). It has been shown that conformational changes followed by binding with heparin-like molecules in the heparin-binding domain is required for maximal HB-EGF activity as a mitogen (*9*). Recently, processing of the N-terminal domain adjacent to the heparin-binding domain by MT1-MMP was shown to convert HB-EGF to a heparin-independent mitogen (*10*).

HB-EGF is involved in several physiological and pathological processes. Analyses of *Hbegf*-null mice implicated a role in the maintenance of heart muscle, formation of heart valves, lung development, eyelid formation and wound healing of skin (*11–15*). Human ovarian cancer cell lines form tumours in nude mice when these cells are subcutaneously injected (*16*). Tumour formation by these cells is strongly enhanced by exogenous expression of proHB-EGF, but exogenous expression of an uncleavable form of HB-EGF (*17*) did not induce tumours development (*16*). Tumour formation by these cells was completely blocked by inhibition of HB-EGF gene expression using short interfering RNA (siRNA). These results indicate that sHB-EGF is involved in tumour formation. HB-EGF is also involved in malignancy, and

HB-EGF expression was found to be upregulated in many types of malignant tumours (*16*, *18–21*). In ovarian cancer, HB-EGF expression was increased in advanced cancer compared with normal ovarian tissue and was associated with poor clinical outcome (*16*, *22*). Several lines of evidence indicated that HB-EGF is an early response gene to chemotherapy and contributes to chemotherapy resistance (*23–25*). Thus, HB-EGF is now recognized to be a possible target for cancer therapy.

ProHB-EGF functions as cellular receptor for diphtheria toxin (DT) secreted by *Corynebacterium diphtheriae* (*C.diphtheriae*) on the plasma membrane (*26*, *27*). DT is a single polypeptide chain of 535 amino acids consisting of two subunits, fragments A and B, linked by disulfide bonds (*28*, *29*). Fragment A contains a catalytic (C) domain and fragment B is composed of transmembrane (T) and receptor binding (R) domains (*30*). DT specifically binds to the EGF-like domain of HB-EGF via the R domain (*31*, *32*), and heparin-like molecules facilitate interaction of DT with HB-EGF (*33*). After binding of DT to proHB-EGF, DT is internalized by receptor-mediated endocytosis. Conformational changes of DT take place in an acidic compartment, resulting in the insertion of DT into the endosomal membrane by certain regions in the T domain, and finally, the enzymatically active fragment A is translocated to the cytosol (*34*). Fragment A inhibits cellular protein synthesis in eukaryotes by inactivating elongation factor 2 through ADP ribosylation (*35*).

The DT gene originates from the *tox* gene of *Corynebacterium* phage (*36*, *37*). Cross-reacting material (CRM) 197 is a product of a single missense mutation (G52E) within fragment A, resulting in enzymatically inactive product (*38*, *39*). Although CRM197 had been thought to be a non-toxic mutant protein, further research clarified that CRM197 possesses weak EF2-ADP-ribosyl activity and that it shows cytotoxicity to cells expressing a high level of proHB-EGF on their surface (*40*, *41*). Because CRM197 maintains HB-EGF-binding properties, it inhibits HB-EGF-dependent EGFR activation by sequestering soluble ligand (*16*, *31*) and by attenuating ectodomain shedding of proHB-EGF (*42*). Thus, CRM197 is predicted to inhibit HB-EGF-expressing tumour cells by three modes of action: sequestering of sHB-EGF, inhibition of ectodomain shedding of proHB-EGF and weak DT toxicity. Moreover, CRM197 inhibits tumorigenesis of various cancer cells including ovarian, gastric and breast cancer cells in mice (*16*, *22*, *24*, *43*, *44*) and clinical trials for ovarian cancers using CRM197 are currently in progress.

In this study, we attempted to generate CRM197 derivatives that have higher inhibitory activity for HB-EGF than wild-type (WT) CRM197. We identified four mutations in the R domain with enhanced proliferation inhibitory activity and binding affinity to HB-EGF, and constructed a mutant, CRM197(R460H), that carries a newly identified mutation.

Materials and Methods

Reagents

Recombinant HB-EGF and TGF-α were obtained from R&D Systems (MN, USA). C-terminally Myc- and His-tagged soluble form of human HB-EGF lacking amino acids 93–104 of heparin-binding domain (sΔHB-mycHis) proteins (*9*) were collected and purified from the conditioned medium (CM) of transfected HEK293 cells by using TALON metal affinity resin. Briefly, CM containing sΔHB-mycHis proteins was bufferized with 20 mM 4-(2-Hydroxyethyl)-1-piperazineethane-sulfonic acid (HEPES)–NaOH pH7.2, and incubated with TALON gel for over-night at 4°C. After washing the gel with phosphate buffered saline (PBS: 10 mM Na_2HPO_4, 2 mM KH_2PO_4, 2.7 mM KCl, 137 mM NaCl, pH 7.4), sΔHB-mycHis proteins were eluted with the elution buffer (PBS containing additionally 150 mM NaCl and 150 mM imidazole). Eluted fractions were determined by immunoblotting using anti-myc tag mAb 9E10. Then the eluate was dialysed against PBS. Actual concentration of the yielded sΔHB-mycHis proteins was determined by judging the purity of the sΔHB-mycHis protein with densitometry of silver-stained gel after electrophoresis in total protein content measured with Bradford method.

Cell culture

DER cells were established by introducing exogenous human EGFR cDNA into bone marrow-derived lymphoblastic 32D cells (*45*). DER cells were maintained as described previously (*45*). Buffalo rat liver (BRL) cell and BRL cells expressing exogenous human HB-EGF (BRLH) were established and maintained as described previously (*8*).

Glutathione-S-transferase-fusion R domain

cDNA of the entire R domain (residues 380–535) amplified by polymerase chain reaction (PCR) was inserted into the BamHI-EcoRI sites of pGEX-3 vector (GE Healthcare) and transformed into *Escherichia coli* JM109. A single colony was inoculated into 40 ml of LB medium containing 50 μg/ml ampicillin (LB-amp) and incubated overnight at 37°C. The pre-culture medium was inoculated into 500 ml of fresh LB-amp and grown at 37°C until the bacterial logarithmic proliferation phase was reached. glutathione-S-transferase (GST)-R domain was induced with 0.4 mM isopropyl β-D-1-thiogalactopyranoside (IPTG) for 2 h at 37°C. Cells were collected by centrifugation and washed with solution A (20 mM Tris–HCl, pH8.0, 30 mM NaCl, 10 mM ethylenediaminetetraacetic acid) containing 0.2 mM phenylmethylsulfonyl fluoride (PMSF). Cells were collected again by centrifugation and lysed with solution A containing lysozyme (40 μg/ml) on ice for 1 h. Cell lysate was further incubated for 15 min on ice after addition of Triton-X100 (0.53%) and NaCl (100 mM). Cell lysates were sonicated for 20 s (twice on ice) in the presence of the 0.2 mM PMSF and then cleared by centrifugation. The supernatant was incubated with Glutathione-Sepharose 4B (GE Healthcare) overnight at 4°C. Beads were washed with solution A, and bound protein was eluted with elution buffer (100 mM Tris–HCl, pH 8.0, 6 mM glutathione).

Thioredoxin-fusion R domain

cDNA of R domain was cloned into the XhoI-EcoRI sites of pThioHis vector (Invitrogen, CA, USA) and transformed into *E.coli* JM109. ThioHis-fusion protein was purified according to manufacturer's instruction using the His-Patch ThioFusion Expression System (Invitrogen).

MBP-fusion R domain

R domain cDNA was cloned into the BamHI-*Pst*I sites of pMAL-p2 vector (New England BioLabs Inc., MA, USA) and transformed into *E.coli* JM109. Primers used for PCR were as follows (restriction enzyme sites for cloning are underlined): Fw, 5′-GCAGGATCCCC CGCGTATTCTCCGGGG-3′, Rv, 5′-CGCTGCAGTCAGCTTTT GATTTCTAG-3′. To separate the R domain from maltose-binding protein (MBP), oligonucleotide encoding PreScission Protease (GE Healthcare) recognition sequence (LEVLFQ/GP) was inserted into the BamHI site of pMAL-p2 vector. A single colony was inoculated into 40 ml of LB-amp and grown for overnight at 37°C. Pre-culture was inoculated into 500 ml of fresh LB-amp and cultured at 37°C until the logarithmic proliferation phase was reached. MBP-fusion protein was induced with 1 mM IPTG for 3 h at 37°C. Cells were

collected by centrifugation and washed with solution B (20 mM HEPES, pH 7.3, 150 mM NaCl). Cells were collected again by centrifugation, re-suspended in solution B, and disrupted by sonication. Cell lysate was cleared by centrifugation, and the supernatant was mixed with Amylose Resin (New England BioLabs) overnight at 4°C. Resin was washed with solution B, and bound protein was eluted in solution B containing 100 mM maltose. Fusion protein was incubated with PreScission Protease, and MBP and PreScission Protease were removed by incubation with Amylose Resin and Glutathione-Sepharose 4B, respectively. Protein concentration of purified MBP-R domain proteins were determined by Coomassie Brilliant Blue methods.

MBP-R domain mutants

MBP-R domain mutants were constructed by site-directed mutagenesis using PCR. Oligonucleotides used for mutant construction are listed in Table I. PCR products treated with DpnI were transformed into *E.coli* JM109. Nucleotide sequences of mutants were verified by DNA sequencing. MBP-R domain mutants were purified as described above. Protein content of purified MBP-R domain mutants was measured with Bradford method.

Proliferation inhibition assay

DER cells (1×10^4 cells) were cultured in RPMI1640 medium containing 10% fetal bovine serum (FBS), recombinant HB-EGF (10 ng/ml), heparin (10 μg/ml), penicillin G (100 U/ml) and streptomycin (100 μg/ml) (*9*) for 40 h in the presence or absence of various concentrations of MBP-R domain proteins. Concentrations of MBP-R domain proteins were 0.22, 0.67, 2, 6.1, 18.5, 55.5 and 167 nM. Culture was performed in 96-well plates (100 μl medium/well). The number of DER cells was measured by Cell Count Reagent SF (Nacalai Tesque, Japan) according to the manufacturer's instructions. All experiments were carried out in duplicate or triplicate, and the data were presented as the mean ± SD obtained by total 4–8 samples.

Collagen gel culture

Ice-cold bovine type I collagen (Nitta Gelatin; 3 mg/ml), reconstitution buffer comprising 2.2% (w/v) $NaHCO_3$, 0.2 M HEPES and 50 mM NaOH, 10×DMEM (Dulbecco's modified Eagle's medium)-F12 (1:1) medium and cells suspended in serum-free DMEM (5×10^6 cells/ml) were mixed in an 8:1:1:0.1 ratio and poured into 24-well dishes (0.5 ml/well) as described previously (*8*). After a 30-min incubation at 37°C, collagen gels were overlaid with 1 ml DMEM-FBS containing either CRM197, MBP-R(WT) or MBP-R(mutant), and cultured for 1 week. To count cell number, the collagen gels were incubated with 0.5 ml of 0.5% (w/v) bacterial collagenase (Invitrogen) in HBS (+) (10 mM HEPES, pH7.2, 140 mM NaCl, 4 mM KCl, 1.8 mM $CaCl_2$ and 1 mM $MgCl_2$) at 37°C until they dissolved, and the cells were then harvested by centrifugation. Cells were fixed and stained with crystal violet solution (0.1% crystal violet, 0.1 M citric acid), and the number of nuclei was counted under a microscope after vortexing. All experiments were carried out in triplicate, and the data were presented as the mean ± SD.

Surface plasmon resonance

A Biacore T200 and Sensor Chip NTA (GE Healthcare) were used for this analysis. Coupling constants of HB-EGF and R domain mutants were measured according to the manufacturer's instructions. Briefly, solution C (GE Healthcare) was used as running buffer. Ni^{2+} was first captured on sensor chip at 10 μl/min flow rate for 60 s, and then sΔHB-mycHis was captured for 180 s. Captured sΔHB-mycHis was reacted with five different concentrations of CRM197, MBP-R(WT) or MBP-R(mutant) at 30 μl/min flow rate for 600 s. Dissociation was monitored at 30 μl/min flow rate for 600 s. Ka values were calculated using Biacore Software (GE Healthcare).

Establishment of C.diphtheriae expressing CRM197 mutants by triparental mating

CRM197 gene and its promoter were obtained from *C.diphtheriae* C7hm723 (β197) strain (*46*) genomic DNA by PCR. Primers used were as follows (restriction enzyme sites for cloning are underlined): Fw, 5′-GCGAGATCTTTAGGATAGCTTTACCTAATTATTTTATG-3′, Rv, 5′-CGCCATGCGGCCGCTCAGCTTTTGATTTCAAAAAATAGCG-3′. Amplified DNA was inserted into the *Bgl*II-*Not*I sites of pK-PIM vector (*47*) and transformed into *E.coli* DH10B. CRM197(R460H) mutant was constructed by site-directed mutagenesis using pK-PIM/CRM197 as a template. pK-PIM vector encodes bacteriophage *att*P sites, integrase gene and kanamycin resistance gene. pK-PIM vector can be integrated into the *C.diphtheriae* genome at *att*B sites, and any integrants become kanamycin resistant. *E.coli* HB101/prk2013 is a helper strain that carries prk2013 plasmid encoding *tra* gene, which is required for

Table I. Oligonucleotide sequences used for construction of R-domain mutants.

MBP-R mutants	Fw primer
MBP-R(WT)	gcaggatcccccgcgtattctccgggg
MBP-R(H384K)	cccgcgtattctccggggaaaacgcaaccatttc
MBP-R(H384Y)	gcgtattctccggggtataaaacgcaaccatttc
MBP-R(F389H)	cataaaacgcaaccacatcttcatgacggg
MBP-R(F389K)	cataaaacgcaaccaaaacttcatgacggg
MBP-R(F389Q)	cataaaacgcaaccacagcttcatgacggg
MBP-R(F389R)	cataaaacgcaaccacgccttcatgacggg
MBP-R(F389Y)	ataaaacgcaaccatatcttcatgacggg
MBP-R(H391C)	caaccatttctttgcgacgggtatgctg
MBP-R(H391D)	caaccatttcttgatgacgggtatgctg
MBP-R(H391E)	caaccatttcttgaagacgggtatgctg
MBP-R(H391G)	caaccatttcttggcgacgggtatgctg
MBP-R(H391K)	caaccatttcttaaagacgggtatgctgtc
MBP-R(R460H)	cggaaaataaggatgcattgcagagctatagac
MBP-R(R460K)	cggaaaataaggatgaaatgcagagctatagac
MBP-R(R462H)	ggatgcgttgccatgctatagacgg
MBP-R(R462K)	ggatgcgttgcaaagctatagacgg
MBP-R(R472H)	gtaacttttttgtcatcctaaatctcctg
MBP-R(R472K)	gtaacttttttgtaaacctaaatctcctg
MBP-R(R472Q)	gtaacttttttgtcagcctaaatctcctg
MBP-R(D507A)	gaaatttcgtcggcgtccataggcgttc
MBP-R(D507H)	gaaatttcgtcgcattccataggcgttcttggg
MBP-R(D507N)	gaaatttcgtcgaactccataggcgttc
MBP-R(Q515E)	ggcgttcttgggtacgaaaaaacagtagatcac
MBP-R(Q515N)	ggcgttcttgggtacaacaaaacagtagatcac
MBP-R(K516H)	gttcttgggtaccagcatacagtagatcac
MBP-R(K516R)	gttcttgggtaccagcgcacagtagatcac
MBP-R(D519E)	cagaaaacagtagaacacaccaagg
MBP-R(D519I)	cagaaaacagtaattcacaccaagg
MBP-R(D519L)	cagaaaacagtactgcacaccaagg
MBP-R(D519N)	cagaaaacagtaaaccacaccaagg
MBP-R(D519Q)	cagaaaacagtacagcacaccaagg
MBP-R(D519V)	cagaaaacagtagtgcacaccaagg
MBP-R(H520K)	cagaaaacagtagataaaaccaaggttaattctaag
MBP-R(H520R)	cagaaaacagtagatcgcaccaaggttaattc
MBP-R(N524D)	cacaccaaggttgattctaagctatcg
MBP-R(N524Q)	cacaccaaggttcagtctaagctatcg
MBP-R(K526H)	ggttaattctcatctatcgctatttttg
MBP-R(K526G)	cacaccaaggttaattctggcctatcgctatttttg
MBP-R(K526R)	ccaaggttaattctcgcctatcgctatttttg
MBP-R(S528H)	gttaattctaagctacatctatttttgaaatc
MBP-R(S528K)	gttaattctaagctaaaactatttttgaaatc
MBP-R(S528N)	gttaattctaagctaaacctatttttgaaatc
MBP-R(S528Q)	gttaattctaagctacagctatttttgaaatc
MBP-R(S528T)	gttaattctaagctaaccctatttttgaaatc
MBP-R(F530H)	ctaagctatcgctacatttgaaatcaaaagc
MBP-R(F530K)	ctaagctatcgctaaaatttgaaatcaaaagc
MBP-R(F530N)	ctaagctatcgctaaactttgaaatcaaaagc
MBP-R(F530Q)	ctaagctatcgctacaatttgaaatcaaaagc
MBP-R(F530R)	ctaagctatcgctacgctttgaaatcaaaagc
MBP-R(D392G)	caaccatttcttcatggcgggtatgctgtc
MBP-R(G466D/ D467A/V468T)	cgttgcagagctatagacgatgcgaccacttttt gtcgccctaaatc
MBP-R(G466D)	cagagctatagacgatgatgtaacttttgtcgc
MBP-R(D467A)	cagagctatagacggtgcggtaacttttgtcgc
MBP-R(V468T)	cagagctatagacggtgataccacttttgtcgc
MBP-R(I504T/S505P/ S506L/D507S)	gagaaaattcattctaatgaaaccccgctgagct ccataggcgttcttggg
MBP-R(G510D)	cgtcggattccatagatgttcttgggtac

Complementary proves of Fw primers used as reverse primer.

sex pili formation for plasmid transfer. DH10B/pK-PIM, HB101/prk2013, and *C.diphtheriae* were pre-cultured at 37°C overnight. The bacterial density was adjusted to OD600 = 1.0 and mixed at a ratio of DH10B:HB101:*C.diphtheriae* C7(−) = 1:1:8. Pellets of the mixture of bacteria mixture were dropped onto Brain Heart Infusion (BHI) agar plates and incubated at 30°C. *Corynebacterium* cointegrates were diluted with BHI medium, spread on BHI agar plates and incubated at 30°C for 16 h. Colonies were isolated by plating conjugation BHI agar plates containing nalidixic acid (20 μg/ml) and kanamycin (5 μg/ml). To isolate clone of cointegrates, several single kanamycin–resistance colonies were picked independently and grown for 2 days at 30°C. The clones were cultured at 37°C by shaking in BHI medium supplemented with 20 μg/ml nalidixic acid and 5 μg/ml kanamycin. Bacterial pellets were suspended in 100 μl TE buffer and boiled at 96°C for 5 min, and supernatant was used to confirm integration by PCR.

Production and purification of CRM197 and CRM197 mutant

CRM197 and CRM197 mutant were produced and purified as described previously (*37*).

Molecular graphics analysis

The electrostatic molecular surface of HB-EGF is displayed with the crystal structure of the complex of DT and HB-EGF by the molecular graphics program jV (*48*), using the eF-site database for the molecular surface (*49*).

Statistical analysis

The statistical significance was evaluated by Student's *t*-test. Values of $P<0.05$ were considered significant.

Results

Production of recombinant R domain of DT proteins and HB-EGF-inhibitory activity

We constructed and expressed the R domain of DT (R(WT)) fused with distinct expression-purification tags (GST, thioredoxin (TRX) and MBP), and fusion proteins designated GST-R(WT), TRX-R(WT) and MBP-R(WT) were produced and purified by the standard procedures or according to the manufacturer's instructions. Because the MBP-fusion protein was the best for purity and stability among the constructed fusion proteins (data not shown), MBP-R domain was used for further studies.

We first tested whether MBP-R(WT) inhibits HB-EGF-dependent cell proliferation in a DER cell proliferation assay in the presence of recombinant HB-EGF (*42*, *45*). DER cells, which originated from IL-3-dependent 32D cells, stably express human EGFR and can grow in a medium containing EGFR ligands. Without IL-3, DER cell showed EGFR-ligand dependent-cell proliferation. Thus, DER cell proliferation assay in the presence of HB-EGF enables detection of HB-EGF-inhibitory activity of test samples in an HB-EGF-specific manner. MBP-R(WT) inhibited the proliferation of DER cells in a dose-dependent manner (Fig. 1A). However, its inhibitory activity was lower than that of CRM197; ID_{50} values, determined by the concentration at which cell numbers are decreased by 50%, were 1.2 and 7.9 nM for CRM197 and MBP-R(WT), respectively. It seemed to be plausible that the lower inhibitory activity of MBP-R(WT) was caused by the steric hindrance of the MBP tag to the interaction of R domain with HB-EGF; however, this was not case. We removed the MBP tag from MBP-R(WT) by PreScission Protease and purified R(WT). R(WT) and MBP-R(WT) showed similar

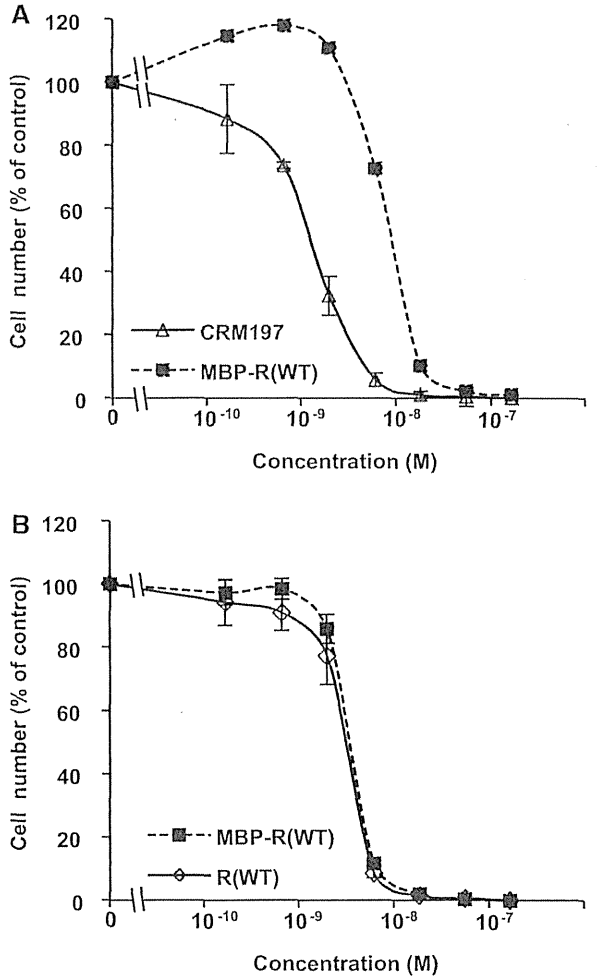

Fig. 1 Inhibition of HB-EGF-dependent proliferation of DER cells by CRM197 or recombinant R domain proteins. DER cells stimulated with HB-EGF were cultured in the presence of various concentrations of CRM197 or recombinant R domain proteins for 40 h and cell number was counted. (**A**) Comparison of CRM197 and MBP-R(WT). (**B**) Comparison of MBP-R(WT) and R(WT).

inhibitory activity (Fig. 1B), indicating that the MBP tag does not interfere with the inhibitory activity of R domain.

Design of R domain mutants

To obtain R domain mutants with higher inhibitory activity than R(WT), we produced various MBP-R domain mutants in which an amino acid residue was substituted with other amino acid residues by site-directed mutagenesis. We chose amino acid residues for substitution using the following criteria: (i) residues that are expected to interact directly with HB-EGF, based on data obtained from the X-ray crystal structure of the DT/HB-EGF complex (*50*) and a molecular graphics analysis or (ii) residues that are known to be important for HB-EGF binding (*51*). MBP-R domain mutants constructed in this study are listed in Table II and mutated residues in R domain are shown in Fig. 2.

The rationales for the mutation of each amino acid residue are described as follows.

Table II. MBP-R mutants with single amino acid substitution and their inhibitory activity.

MBP-R mutants	ID50(nM)[a]
CRM197	1.2
MBP-WT	7.9
MBP-R(H384K)	7.6
MBP-R(H384Y)	8.0
MBP-R(F389H)	12
MBP-R(F389K)	42
MBP-R(F389Q)	27
MBP-R(F389R)	38
MBP-R(F389Y)	66
MBP-R(H391C)	21
MBP-R(H391D)	84
MBP-R(H391E)	68
MBP-R(H391G)	18
MBP-R(H391K)	2.4
MBP-R(R460H)	2.8
MBP-R(R460K)	7.8
MBP-R(R462H)	8.0
MBP-R(R462K)	8.6
MBP-R(R472H)	23
MBP-R(R472K)	4.0
MBP-R(R472Q)	56
MBP-R(D507A)	14
MBP-R(D507H)	55
MBP-R(D507N)	4.5
MBP-R(Q515E)	8.0
MBP-R(Q515N)	16
MBP-R(K516H)	84
MBP-R(K516R)	26
MBP-R(D519E)	10
MBP-R(D519I)	16
MBP-R(D519L)	12
MBP-R(D519N)	9.0
MBP-R(D519Q)	17
MBP-R(D519V)	25
MBP-R(H520K)	6.0
MBP-R(H520R)	8.6
MBP-R(N524D)	>167
MBP-R(N524Q)	40
MBP-R(K526H)	16
MBP-R(K526G)	>167
MBP-R(K526R)	9.9
MBP-R(S528H)	21
MBP-R(S528K)	>167
MBP-R(S528N)	45
MBP-R(S528Q)	22
MBP-R(S528T)	23
MBP-R(F530H)	17
MBP-R(F530K)	13
MBP-R(F530N)	55
MBP-R(F530Q)	10
MBP-R(F530R)	10
MBP-R(D392G)	19
MBP-R(466-468)[b]	2.7
MBP-R(G466D)	9.0
MBP-R(D467A)	8.0
MBP-R(V468T)	6.2
MBP-R(504-507)[c]	>167
MBP-R(G510D)	11

[a]ID_{50} was calculated by the data of Figs 1, 4 and Supplementary Figs 1 and 2.
[b]G466D/D467A/V468T.
[c]I504T/S505P/S506L/D507A.

H384. H384 is reported to interact with HB-EGF S147 via a salt bridge (*50*); it was replaced with K, which has a strong positive charge. H384 was also replaced with Y because the polar long side chain of Y was expected to contact more closely with HB-EGF than H.

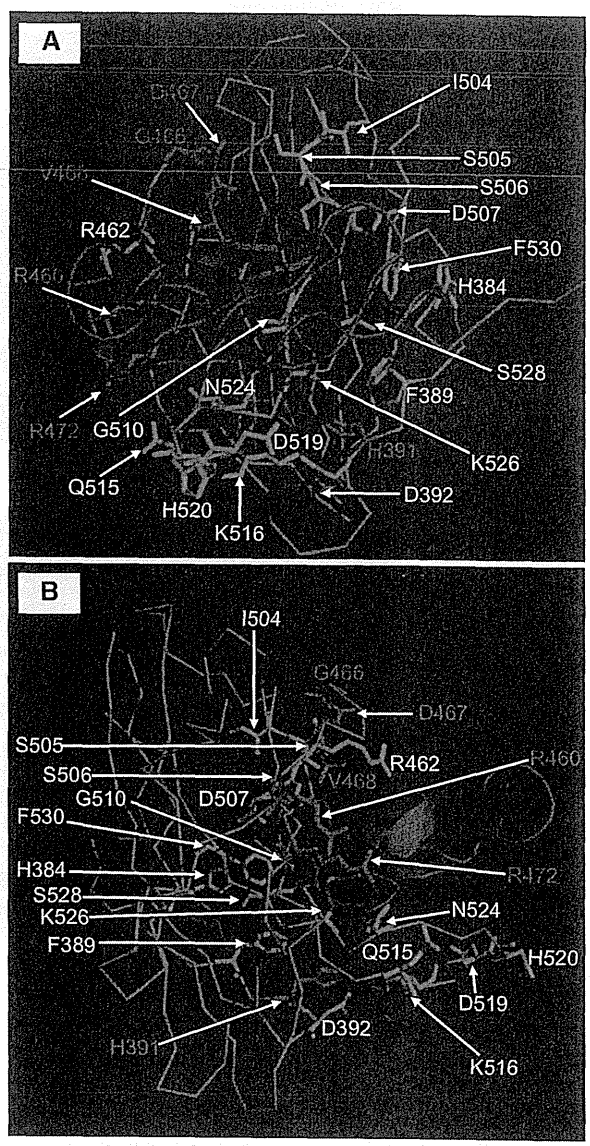

Fig. 2 Substituted amino acids. Steric structure of DT R domain (brown) and EGF-like domain of HB-EGF (green) are shown from the crystal structure of the complex of DT and HB-EGF (PDBID: 1XDT). Mutated (substituted) amino acid residues in this study are shown with their side chains. Amino acid residues whose substitutions to another residues resulted in higher inhibitory activity to HB-EGF are shown in red, and those did not are in purple. (**A**) top view; (**B**) side view.

F389. F389 indirectly interacts with HB-EGF via water molecules; replacement with hydrophilic amino acids (H, K, Q, R, Y) was expected to increase affinity to HB-EGF by establishing direct interaction.

H391. H391 was reported to interact with E141 of HB-EGF via a salt bridge (*50*) (Fig. 3). Therefore, H391 was replaced with K. For control mutants, H391 was also replaced with non-polar (G), neutral polar (C) and acidic polar (D, E) amino acids.

R460. This region constitutes the P site, which has been shown to function in phosphate binding and to affect the interaction of DT with HB-EGF (*52*). It was replaced with basic amino acids (H, K) (Fig. 3).

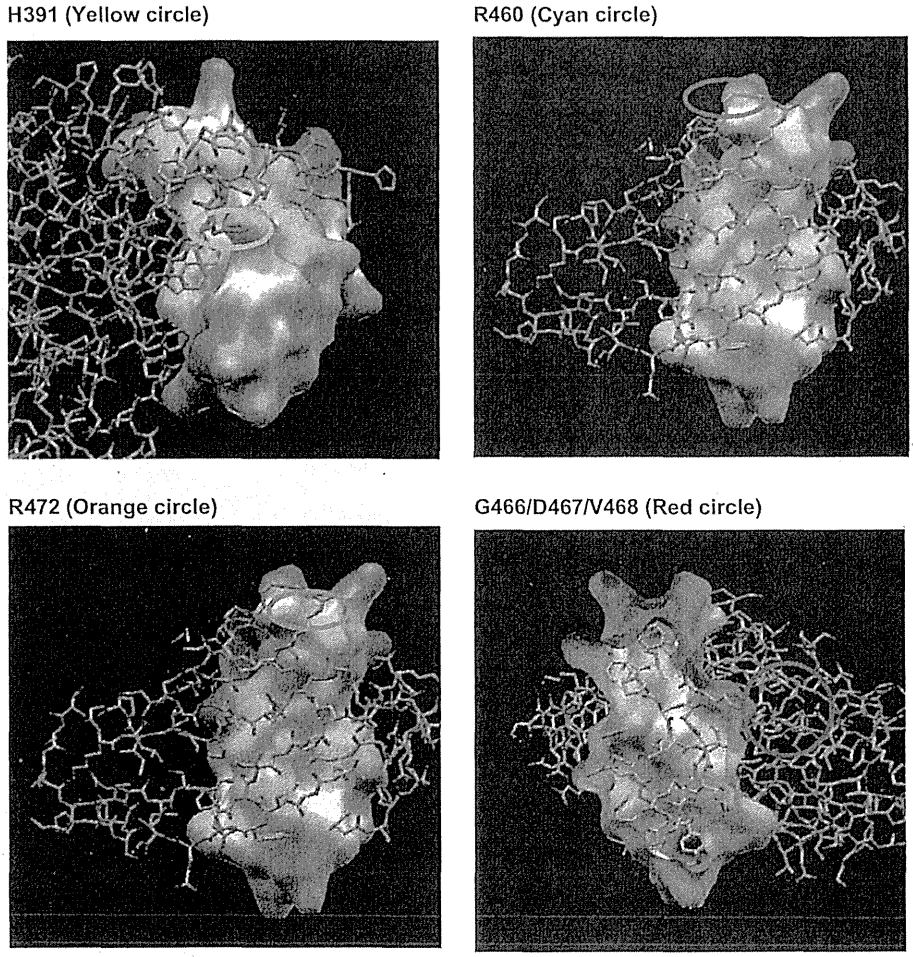

Fig. 3 Interactions between DT R domain and HB-EGF EGF-like domain. Electrostatic molecular surface of the EGF-like domain of HB-EGF is shown with the atomic structure of the DT R domain (PDBID: 1XDT), using the eF-site database (*49*). Blue and red surface colours correspond to positive and negative electrostatic potentials, respectively, and yellow colour indicates where the hydrophobic side-chain appears on the surface. H391, R460, R472, G466/D467/V468 are indicated by coloured circles.

R462. R462, reported to interact with HB-EGF E126 via salt bridge (*50*), was replaced with basic amino acids (H, K).

R472. According to an analysis of electrostatic complementarity between the R domain and HB-EGF, replacement of R472 with Q was expected to increase binding with HB-EGF (Fig. 3). R472 was also replaced with basic amino acids (H, K).

D507. According to the X-ray crystal structure (*50*) and molecular graphics analysis, D507 is repulsive for the negatively-charged HB-EGF interface. Therefore, D507 was replaced with neutral amino acids (A, N) or a basic amino acid (H).

Q515. Q515 contacts with HB-EGF S127, which is known to be essential for DT binding. Therefore, it was replaced with a hydrophilic amino acid (N) or acidic amino acid (E).

K516. K516 was reported to interact with E141 of HB-EGF via a salt bridge and be important for binding with HB-EGF (*51*). We expected that substitution with positively-charged amino acids (H, R) might increase affinity.

D519. Because D519 contacts with HB-EGF R142, D519 was replaced with an acidic amino acid (E). As control mutants, D519 was also replaced with hydrophobic amino acids (I, L, V) or hydrophilic amino acids (N, Q).

H520. H520A mutation was reported to decrease binding with HB-EGF (*51*). Therefore, it was replaced with other basic amino acids (K, R) to increase the basic charge.

N524. N524 contacts with HB-EGF L127 via van der Waals forces. N524 was substituted with neutral amino acid Q or negatively charged amino acid D.

K526. K526 is reported to interact with C132 and E141 of HB-EGF via hydrogen bonds (*50*). We replaced K526 with basic amino acids (R, H). K526 was also replaced with G as a control.

S528. Because S528 was reported to indirectly interact with HB-EGF G140 though water molecules (50), it was substituted with hydrophilic amino acids (N, Q, T) or basic amino acids (H, K).

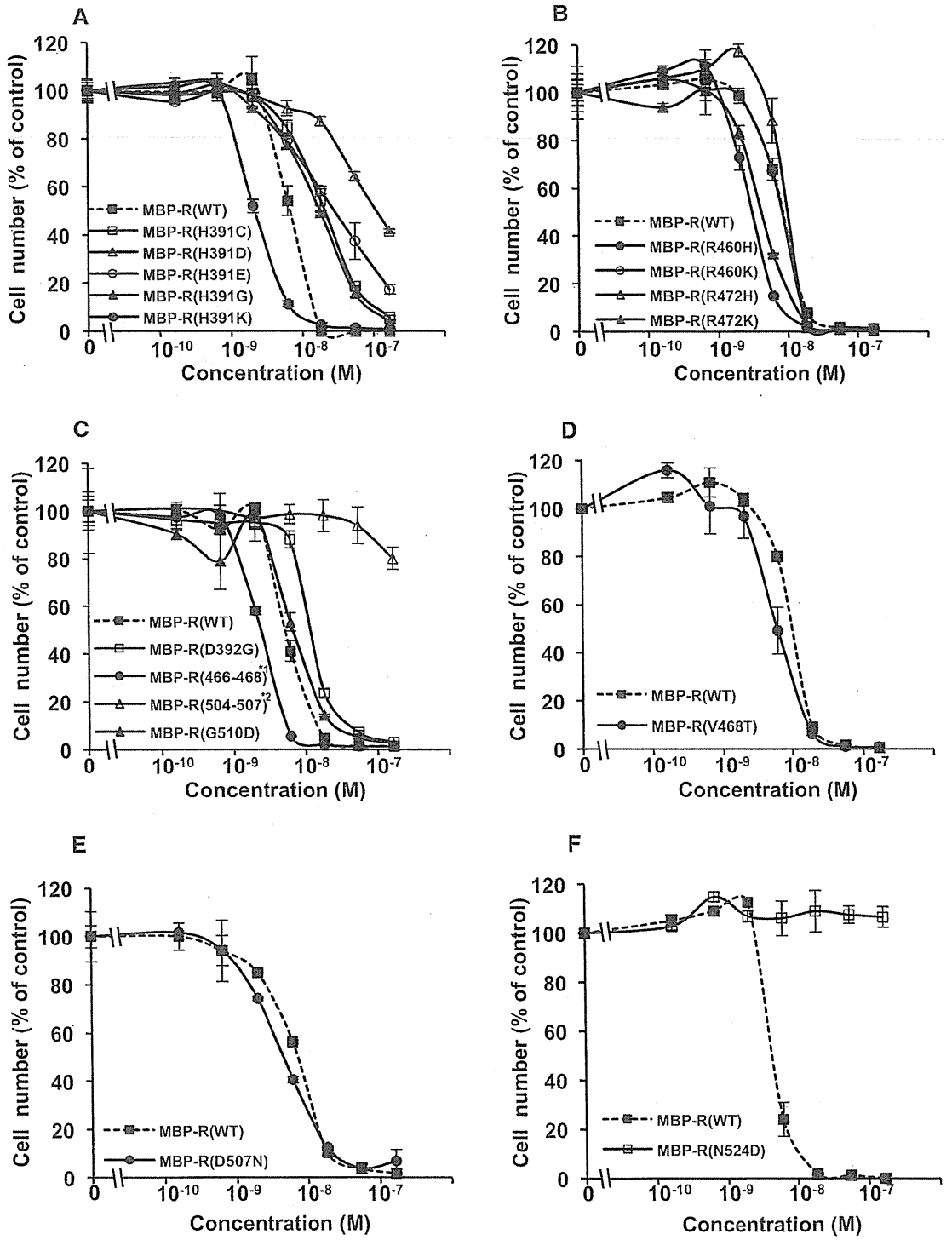

Fig. 4 Inhibition of HB-EGF-dependent proliferation of DER cells by MBP-R mutants. DER cells stimulated with HB-EGF were cultured in the presence of various concentrations of MBP-R(WT) or MBP-R mutants for 40 h and cell number was counted. (**A**) H391 mutants. (**B**) R460 and R472 mutants. (**C**) *C. ulcerans*-type mutants. (**D**) V468T mutant. (**E**) D507N mutant. (**F**) N524D mutant.

F530. Because F530A mutation was reported to reduce affinity to HB-EGF (*51*), F530 was replaced with basic amino acids (H, K, R) or hydrophilic amino acids (N, Q).

D392G, G466D/D467A/V468T, G466D, D467A, V468T, I504T/S505P/S506L/D507S and G510D. C. ulcerans produces diphtheria-like toxin (DLT) (*53*). DLT shows higher binding affinity to human HB-EGF than DT (unpublished observation by Dr. Yukiji Seto). DLT has some differences in amino acid sequence compared with that of DT around the HB-EGF binding interface (D392, G466/D467/V468, G466, D467, V468, I504/S505/S506/D507, G510). Therefore, these amino acid residues were replaced with the corresponding amino acid residues of DLT.

Inhibitory activity of R domain mutants and identification of R domain mutants with increased inhibitory activity

To assess the inhibitory activity of R domain mutants against HB-EGF mitogenic activity, DER cells stimulated with HB-EGF were cultured in the presence of R domain mutant proteins. Representative data are shown in Fig. 4, Supplementary Figs S1 and S2. Most mutants showed no apparent change in inhibitory activity, while some mutants largely reduced the inhibitory activity, for example MBP-R(N524D) mutant (Fig. 4F). All ID_{50} values of MBP-R mutants tested are listed in Table II.

Among the R domain mutant proteins tested, nine mutant proteins showed higher inhibitory activity than MBP-R(WT). The ID_{50} value of each mutant compared with CRM197 was as follows: CRM197, 1.2 nM; MBP-R(H384K), 7.6 nM; MBP-R(H391K), 2.4 nM; MBP-R(R460H), 2.8 nM; MBP-R(R460K), 7.8 nM; MBP-R(R472K), 4.0 nM; MBP-R(D507N), 4.5 nM; MBP-R(H520K), 6.0 nM; MBP-R(G466D/D467A/V468T), 2.7 nM; MBP-R(V468T), 6.2 nM; MBP-R(WT), 7.9 nM. We selected upper four mutant proteins, MBP-R(H391K), MBP-R(R460H), MBP-R(R472K) and MBP-R(G466D/D467A/V468T) for further analysis. Direct comparisons of the inhibitory activity of four mutants are shown in Fig. 5.

To examine whether the inhibitory activity of these R domain mutants was specific for HB-EGF, DER cells were cultured in the presence of TGF-α and R domain mutants. None of these mutants affected the proliferation of DER cells (Fig. 6), suggesting that these R domain mutant proteins specifically inhibited HB-EGF without any cytotoxicity.

Effect of the four R domain mutants on HB-EGF-dependent cell proliferation in three-dimensional culture

HB-EGF preferentially stimulates proliferation of adherent cells in three-dimensional (3D)-culture conditions (*8*). We therefore examined the inhibitory activity of the four R domain mutants for HB-EGF-dependent proliferation of BRL cells under 3D-culture conditions using 3D-collagen gel. The four R domain mutants, MBP-R(H391K), MBP-R(R460H), MBP-R(R472K), MBP-R(G466D/D467A/V468T) inhibited BRL cell proliferation induced by recombinant HB-EGF more effectively than MBP-R(WT) (Fig. 7A–C). Moreover, these mutants also inhibited proliferation of BRLH cells, which overexpress exogenous proHB-EGF (Fig. 7D and E). These results strongly suggest that the higher inhibitory activity of the four R domain mutants compared with MBP-R(WT) was not specific for certain cell types or culture conditions.

Affinity constants of R domain mutants against HB-EGF

To examine whether the four R domain mutants had acquired increased affinity against HB-EGF compared with the WT R domain, the affinity constants of the mutants were calculated using a Biacore, according to the manufacturer's instructions. We measured binding of MBP-R domain proteins against recombinant

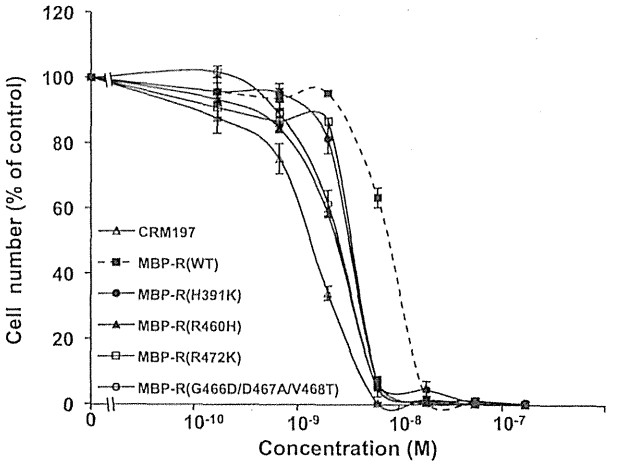

Fig. 5 Comparison of MBP-R mutants with increased inhibitory activity. DER cells stimulated with HB-EGF were cultured in the presence of various concentrations of MBP-R(WT), MBP-R(H391K), MBP-R(R460H), MBP-R(R472K) or MBP-R(G466D/D467A/V468T) mutants for 40 h and cell number was counted.

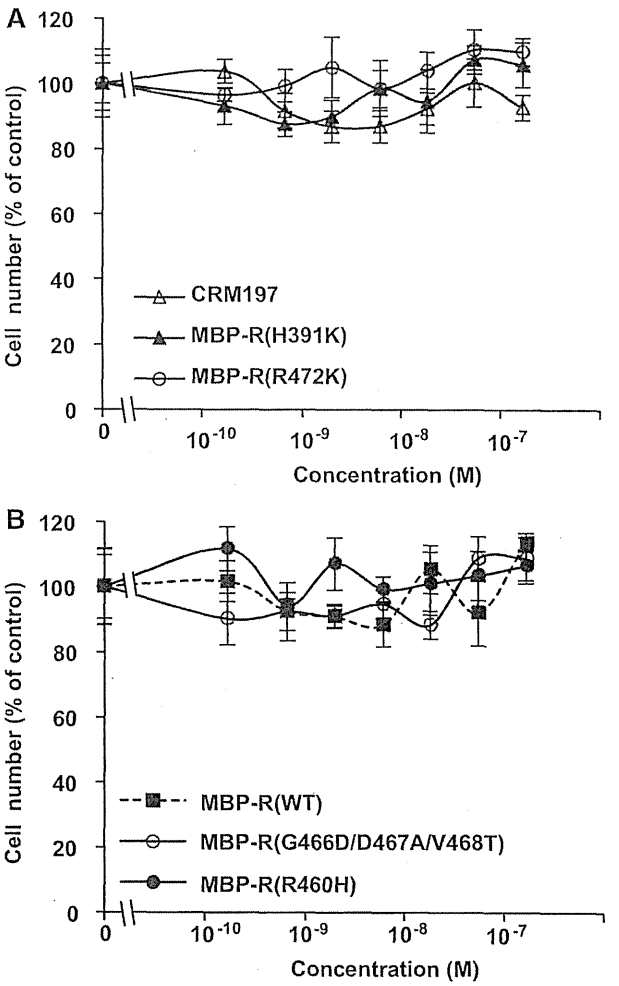

Fig. 6 Effect of CRM197 or MBP-R mutants on TGFα-dependent proliferation of DER cells. DER cells stimulated with TGFα (3 ng/ml) were cultured in the presence of various concentrations of CRM197, MBP-R(WT) or MBP-R mutants and cell number was counted.

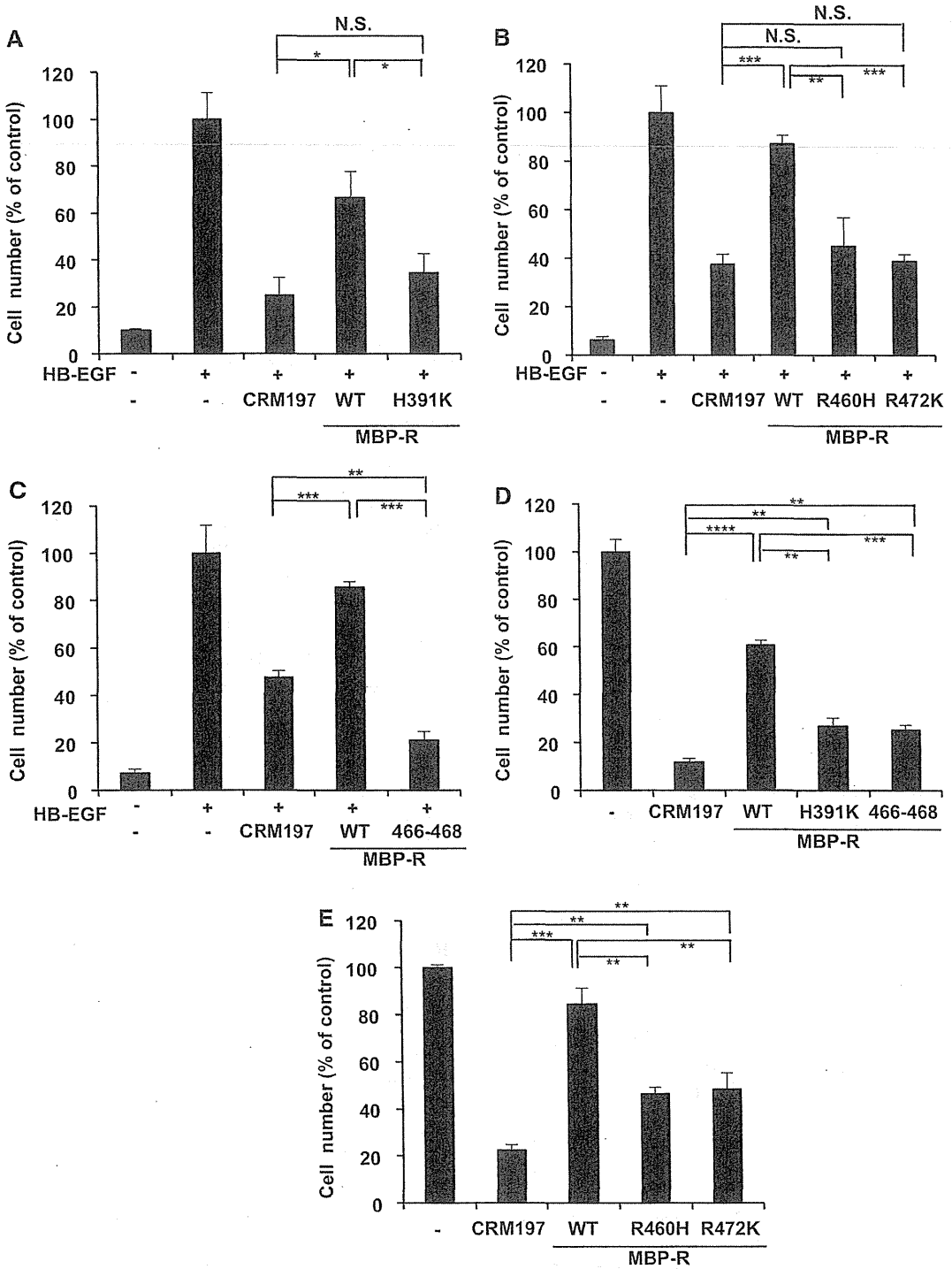

Fig. 7 Inhibitory activity of R-domain mutants on the proliferation of 3D-cultures of BRL cells and BRLH cells. (**A–C**) Effect of MBP-R mutants on BRL cells stimulated with recombinant HB-EGF. CRM197, MBP-R(WT) or MBP-R mutants (5 μM each) and recombinant HB-EGF (30 ng/ml) were added to culture medium and cultured under 3D conditions. (**D, E**) Effect of MBP-R mutants on BRLH cell proliferation. BRLH cells were cultured in the presence of 5 μM of each protein. 466–468, (G466D/D467A/V468T). N.S., not significant. $^{*}P<0.05$, $^{**}P<0.005$, $^{***}P<0.0005$.

HB-EGF captured on a sensor chip, and calculated the affinity constants from association rate constants and dissociation rate constants. Affinity constant values of proteins were as follows: CRM197, $9.22\times10^{8}\,M^{-1}$; MBP-R(R460H), $6.09\times10^{8}\,M^{-1}$; MBP-R(G466D/D467A/V468T), $4.44\times10^{8}\,M^{-1}$; MBP-R(R472K), $4.42\times10^{8}\,M^{-1}$; MBP-R(H391K), $3.17\times10^{8}\,M^{-1}$; MBP-R(WT), $2.99\times10^{8}\,M^{-1}$ (Table III). The order of affinity constant values almost correlated with the order of ID_{50} values. These results suggest that increased affinity against HB-EGF caused the inhibitory activity of the four mutants.

Inhibitory activity of CRM197 mutants against HB-EGF

MBP-R(WT) had lower cell proliferation inhibitory activity than full-length CRM197, suggesting the entire molecular structure is necessary for exerting full inhibitory action. Therefore, we attempted to

Table III. Comparison of MBP-R mutants with increased inhibitory activity.

Name	DER cell assay		Biacore	
	ID_{50} (nM)[a]	Relative values	KA (M^{-1})	Relative values
CRM197	1.3	6.2	9.22×10^8	3.1
MBP-R(WT)	8.0	1.0	2.99×10^8	1.0
MBP-R(H391K)	3.1	2.6	3.17×10^8	1.1
MBP-R(R460H)	2.5	3.2	6.09×10^8	2.0
MBP-R(R472K)	3.2	2.5	4.42×10^8	1.5
MBP-R(466-468)[b]	2.6	3.1	4.44×10^8	1.5

[a]ID_{50} was calculated by the data of Fig. 5.
[b]G466D/D467A/V468T.

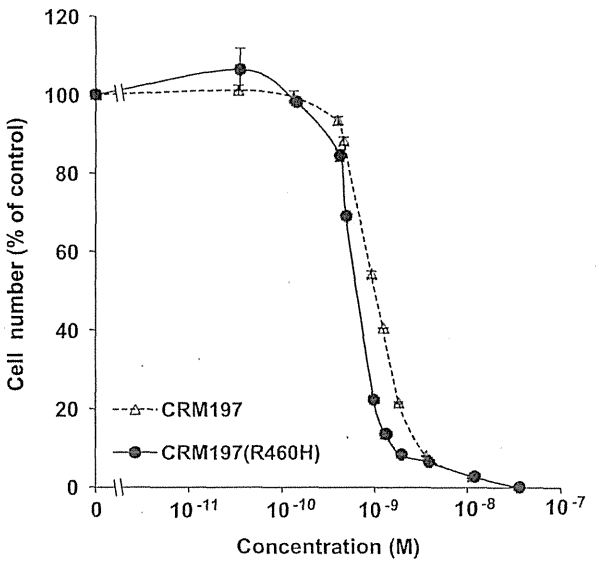

Fig. 8 Inhibition of HB-EGF-dependent proliferation of DER cells by CRM197 mutant. DER cells stimulated with HB-EGF were cultured in the presence of various concentrations of CRM197 or CRM197 (R460H) for 40 h and cell number was counted.

reconstruct and produce full-length CRM197 with R460H mutation in *C.diphtheriae* strains, as described in the Materials and Methods, and compared its inhibitory activity with that of CRM197. CRM197(R460H) significantly inhibited HB-EGF-dependent proliferation of DER cells more efficiently than CRM197(WT) (Fig. 8). The ID_{50} values of CRM197 and CRM197(R460H) were 1.02 nM and 0.72 nM, respectively (Table IV).

To investigate if the affinity constant of CRM197 was improved by the R460H mutation, as observed with the MBP-R domain mutant, we compared the affinity constants of CRM197 and CRM197(R460H) using a Biacore. Affinity constants of CRM197 and CRM197(R460H) were $1.02 \times 10^9 M^{-1}$ and $1.69 \times 10^9 M^{-1}$, respectively (Table IV). Taken together, these results suggested that the inhibitory activity of CRM197 to HB-EGF could be enhanced by mutagenesis.

Discussion

To obtain CRM197 derivatives that have much higher potential of inhibiting the mitogenic activity of

Table IV. Comparison of CRM197 and CRM197(R460H).

Name	DER cell assay		Biacore		
			KA (M^{-1})		
	ID_{50} (nM)[a]	Relative values	Exp1	Exp2	Means
CRM197	1.02	1.0	1.24×10^9	0.806×10^9	1.02×10^9
CRM197 (R460H)	0.72	1.42	2.01×10^9	1.37×10^9	1.69×10^9

[a]ID_{50} was calculated by the data of Fig. 8.

HB-EGF than CRM197, we screened various MBP-R domain mutants. We identified four R domain mutants with increased inhibitory activity against HB-EGF caused by the increased affinity to HB-EGF compared with the WT R domain. CRM197 introduced with the R460H mutation exhibited higher inhibitory activity than WT CRM197. This is the first example of DT mutants with enhanced HB-EGF binding ability.

According to the crystal structure of the DT and HB-EGF complex (*50*), DT H391 forms a salt bridge with HB-EGF E141; an H391K substitution was expected to strengthen this interaction (Fig. 3, yellow circle). Substitution of H391 with acidic amino acid residues E or D that would be repulsive for HB-EGF E126 significantly reduced inhibitory activity (Fig. 4A). Moreover, substitution of H391 with neutral residues C and G also reduced inhibitory activity. R460 constitutes the P site, and may not directly interact with HB-EGF. However, it is located in the environment of positive electrostatic potential formed by the basic residues K125 and R128 of HB-EGF, thus R460H could show upregulation of inhibitory activity. R472 is close to the side-chain of E126 of HB-EGF, which could form a salt bridge with a flexible side-chain of R472K. DT D467 was also indicated to form a salt bridge with HB-EGF K122. According to a molecular graphics analysis, it was expected that G466D/D467A/V468T substitution could introduce two new interactions with HB-EGF; a salt bridge between DT G466D and HB-EGF K122, and interaction of DT V468T with the surface of HB-EGF. Therefore, G466D/D467A/V468T mutations might increase inhibitory activity by enhancing strength of salt bridge.

Although the R domain is responsible for binding of DT with HB-EGF, the binding affinity of recombinant R domain was lower than that of CRM197. Since removal of the MBP-tag did not enhance the inhibitory activity, the other domains of DT may contribute to full HB-EGF-binding activity. Thus, the MBP-R mutants showing higher inhibitory activity than MBP-R(WT) still have lower HB-EGF inhibitory activity compared with that of CRM197. However, introduction of the R460H mutation into CRM197 enhanced the inhibitory activity by ~1.4-fold compared with that of CRM197. It has not been clarified why MBP-R(R460H) showed more than 3-fold higher